(Revised MS for es-2010-010175)

Using a modified electrical aerosol detector (MEAD) to predict nanoparticle exposures to different regions of the respiratory tract for workers in a carbon black manufacturing industry

Ying-Fang Wang[1], Perng-Jy Tsai[1,2], Chun-Wan Chen*[3], Da-Ren Chen[4], Der-Jen Hsu[5]*

[1]Department of Environmental and Occupational Health, Medical College, National Cheng Kung University, 138, Sheng-Li Rd., Tainan 70428, Taiwan;

[2]Sustainable Environment Research Center, National Cheng Kung University, 1, University Road, Tainan 70101, Taiwan;

[3]Institute of Occupational Safety and Health, Council of Labor Affairs, 99, Ln. 407, Hengke Rd., Xizhi City, Taipei County 22143, Taiwan;

[4]Department of Energy, Environmental and Chemical Engineering, Washington University in St. Louis, One Brookings Drive, Box 1180, St. Louis, MO 63130, USA;

[5]Department of Safety Health and Environmental Engineering, National Kaohsiung First University of Science & Technology, 1 University Rd., Yenchau, Kaohsiung County 82445, Taiwan

---

***Correspondence author** phone: +886-6-2353535 ext. 5806; fax: +886-6-2752484; e-mails: pjtsai@mail.ncku.edu.tw; or phone: +886-2-2660-7600 ext. 207; fax: +886-2-2660-7730; e-mails: wann@mail.iosh.gov.tw

Abstract

The present study were set out to characterize nanoparticle exposures in three selected workplaces of the packaging, warehouse, and pelletizing in a carbon black manufacturing plant using a newly developed modified electrical aerosol detector (MEAD). For the confirmation purposes, the MEAD results were compared with those simultaneously obtained from a nanoparticle surface area monitor (NSAM) and a scanning mobility particle sizer (SMPS). We found that workplace background nanoparticle concentrations were mainly coming from the outdoor environment. Size distributions of nanoparticles for the three selected process areas during the work hours were consistently in the form of bi-model. Unlike nanoparticles of the second mode (simply contributed by the process emissions), particles of the first mode could be also contributed by the forklift exhaust or fugitive emissions of heaters. The percents of nanoparticles deposited on the alveolar (A) region were much higher than the other two regions of the head airway (H), tracheobronchial (TB) for all selected workplaces in both number and surface area concentrations. However, significant differences were found in percents of nanoparticles deposited on each of the three regions while different exposure metrics were adopted. Both NSAM and MEAD obtained quite comparable results. No significant difference can be found between the results obtained from SMPS and MEAD after being normalized. Considering the MEAD is less expensive, less bulky, and easy to use, our results further support the suitability of using MEAD in the field for nanoparticle exposure assessments.

Keywords: Nanoparticle exposure, number concentration, surface are concentration, lung deposition, modified electrical aerosol detector, carbon black

Running Title: Assessing nanoparticle exposures in a carbon black industry

Outline of Section Headers

Introduction

Nanoparticles are known for particles with diameters less than 0.1 μm (or 100 nm) (*1*). Nanoparticles might cause serious inflammation after being deposited in the deep lung because of their large particle numbers, surface areas, chemical compositions, sizes, shapes and charges (*2-4*). Recent toxicological studies have suggested that a small fraction of deposited nanoparticles can penetrate cells or tissue and result in many irreversible health effects, such as the chronic pulmonary inflammation, epithelial cell hyperplasia, cardiovascular disease, and lung tumor (*2, 5-7*). To date, both exposure metrics of the total surface area and total number concentrations of nanoparticles have been shown good correlations with their resultant health effects (*3, 8-12*). In addition, health effects associated with nanoparticle exposures are also affected by their regional deposition sites of the respiratory tract. For example, nanoparticles deposit on the alveolar region might interact with epithelial cells and cause inflammation (*13*). Therefore, simultaneously predicting both the total surface area and total number concentrations of nanoparticles deposited on different regions of the respiratory tract is considered a better approach for characterizing nanoparticle exposures. Moreover, the deposition of nanoparticles in the lung is known affected by both their size distributions and human breathing patterns. Therefore, to describe the percent of nanoparticles deposited on different regions of the respiratory tract under a specific breathing pattern (=concentration of nanoparticles deposited on a given region of the lung/total concentration of nanoparticles deposited in the lung) would be important to illustrate the effect of a nanoparticle size distribution on lung deposition.

To date, the scanning mobility particle sizer (SMPS) has been widely used to measure the number concentrations of nanoparticles of different particle sizes in the lab and field (*14*). Although the aforementioned device can neither be used to directly measure their surface area concentrations, nor to estimate exposure concentrations in different regions of the respiratory tract (including the head airway (H), tracheobronchial (TB) and alveolar (A) regions), all of this can be done using predictive particle deposition models and converting the measured mass and/or number concentration to the surface area concentration. Although the combination of a condensation particle counter (CPC), a

74 mass concentration monitor (MCM) and an electrical aerosol detector (EAD) can be used to directly
75 evaluate the surface area concentration of nanoparticle exposures (*15*), the above combination might
76 not be feasible for workplace measurements due to their large volume. Recently, a nanoparticle
77 surface area monitor (NSAM; TSI Inc., Model 3550, St. Paul, MN, USA) has been developed, based
78 on the particle charging characteristics of an EAD, for directly measuring surface area concentrations
79 of nanoparticles deposited on both TB and A regions of the respiratory tract (*16-17*). However, it
80 should be noted that the above instrument can neither simultaneously measure the surface area
81 concentration of the H region, nor the number concentrations of the H, TB, and A regions. More
82 recently, a modified EAD (MEAD) has been developed by our research group to overcome the above
83 mentioned shortcomings (*18-19*). The configuration of the MEAD is similar to that of electrical
84 mobility analyzer of the early generation for particle size distribution measurement. It is therefore
85 possible to use the MEAD as a particle sizer by setting its ion trap at voltages ranging from 20 to 2500
86 V. A data-reduction scheme is used to retrieve the size distribution of sampled particles (assumed as
87 log-normal) from the MEAD readout at different ion-trap voltages. Finally, the built-in programs can
88 be used to directly estimate both the number and surface area concentrations of nanoparticles
89 deposited on different regions of the respiratory tract (including H, TB and A regions) (*18*). It is
90 noteworthy that the aforementioned equipment has never been used in the field. Therefore, the
91 applicability of MEAD in the workplace is still required further confirmation.

92 Carbon black is an important commodity for a wide range of industrial applications. For centuries,
93 carbon black has been mainly used as a pigment for the manufacturing of printing inks, paints, and
94 lacquers. However, its use has been switched as one of reinforcing fillers for the manufacturing of
95 vehicle tires during the past 50 years. To date, animal studies have sown that a short-term low-dose
96 exposure to nano-carbon black might cause the inflammatory reaction (*1, 20-21*). An in vitro study
97 suggests that nano-carbon black exposure can also lead to an increase in the oxidative stress of
98 alveolar epithelial cells (*22*). Another study points out that intranasal instillation of 14 nm carbon
99 black particles might result in the change in brain inflammatory parameters (*23*). To date, carbon

black has not labeled as a known human lung carcinogen by IARC, but has been classified as possibly carcinogenic to human beings (*24*). However, a clear dose/response relationship associated nano-carbon black exposures is still unknown. To date, the release of nano-carbon black to the workplace atmospheres of different manufacturing stages in a carbon black plant have been conducted (*25-27*). However, there is neither number nor surface area of nano-carbon black deposited on different regions of the respiratory tract have been investigated for carbon black manufacturing industries. The aims of the present study were set out first to characterize nano-carbon black exposures for workplaces of different manufacturing stages using the newly developed MEAD. Considering the aforementioned equipment has never been used in the field, the results obtained from MEAD were compared with those simultaneously obtained from NSAM and SMPS for the confirmation purpose.

Material and Methods

Sampling sites. An oil furnace carbon black manufacturing plant located in southern Taiwan was chosen in this study. The manufacturing of carbon blacks involves first the preheating of feedstock oil, air, and gas, and then partial combustion at temperatures ranging from 1,780°C to 1,950°C in the furnace depends on the grade of carbon blacks to be produced. The carbon-rich products (particle size = 10–500 nm, mostly 10–100 nm) are then quenched with water and pass through heat exchangers to recycle the heat for preheating the combustion air. After secondary quenching, the light and fluffy carbon blacks are separated in the bag filter, and then sent through micropulverizers to a surge tank. Finally, the carbon blacks are wet pelletized followed by a drying process to produce pelletized products, and then packaging for shipment (*25*). Detailed manufacturing processes and plant layout can be found in our previous publication (*28*). Three workplaces, including the pelletizing, packaging, and warehouse, were chosen for conducting nanoparticle samplings. Although the packaging area includes two kinds of processes (i.e., the automatic (bulk) packaging and manual packaging), only the manual packaging area was chosen because the other did not have workers in the process area. In

addition, an outdoor sampling site, located at the upwind side of the selected carbon black manufacturing plant, was selected to determine the background nanoparticle concentrations.

Sampling instruments. A MEAD was used to conduct nanoparticle samplings in the present study. The MEAD was installed with a high voltage power supply (Stanford Research Systems Inc., Model PS325/2500V–25W, Sunnyvale, CA, USA) to control the voltages of the ion trap of the EAD (TSI Inc., Model 3070A, St. Paul, MN, USA) varied from 20V–2500V. During samplings, the readings of the electrometer were recorded for each of the eight preset voltages of the ion trap (i.e., 20V, 100V, 200V, 500V, 1000V, 1500V, 2000V, and 2500V. During each sampling run, the sampling time for each preset voltage lasted for ten seconds (*18*). Two reference instruments were used to assess the feasibility of using MEAD in the field. The first one was the NSAM (TSI Inc., Model 3550, St. Paul, MN, USA). This instrument was designed for measuring surface area deposition concentrations of nanoparticles on both TB and A regions of the respiratory tract by setting the ion-trap voltage at 100V and 200V, respectively (*16*). Based on the original design of the NSAM, the readouts are suitable for describing nanoparticle depositions on both TB and A regions for the reference worker under the light exercise mode with nose-only breathing pattern (*17*). The second instrument was the SMPS (TSI Inc., Model 3936, St. Paul, MN, USA) which was used to measure the number concentrations of nanoparticles of different particle sizes with sheath flow 15 L/min, aerosol flow 1.5 L/min and scanning time 300 seconds.

Sampling methods. For each selected workplace, samplings were conducted on consecutive four days. On each sampling day, one MEAD, one NSAM and one SMPS were placed side-by-side, ~1.5 m above the ground level (i.e., the breathing zone), at the location nearest to the main worksite of workers for each selected workplace. For both the packaging area and warehouse, workers only worked from 08:00 AM to 17:00 PM. Therefore, samplings were conducted from 07:00 AM to 08:00 AM and from 10:00 AM to 12:00 AM to determine the workplace concentrations prior to work (denoted as workplace background) and workplace concentrations during the work (denoted as workplace exposure), respectively. Considering workers in the pelletizing area worked for 24 h per

day, samplings were only conducted from 10:00 AM to 12:00 AM for estimating workplace exposure concentrations. No workplace background concentrations of the pelletizing area were measured. For the outdoor sampling site, samplings were conducted from 07:00 AM to 08:00 and 10:00 AM to 12:00 AM to estimate the outdoor atmospheric concentration (denoted as outdoor background).

Data analyses. In the present study, a data-reduction scheme was used to retrieve the size distribution of sampled nanoparticles based on readings obtained the eight preset voltages of the MEAD. Detailed computation processes can be seen in our previous publication (*18*). The resultant size distributions were used to predict depositions of nanoparticles at the H, TB, and A regions of the respiratory tract using the UK National Radiological Protection Board's (NRPB's) LUDEP Software (*29*). The above software was established based on ICRP 66 lung deposition models (*30*). In the present study, we assumed the breathing pattern of workers based on the reference worker parameters can be described as follows:

–Breathing type: nose only

–Functional lung residual capacity: 3301 mL

–Breathing rate: 20 breath/min

–Ventilation rate: 1.5 m^3/h

–Activity level: light exercise.

Fig. 1 shows the predicted deposition curves of the H, TB, and A regions based on the above assumptions. The above criteria were the same as that prescribed for NSAM (*17*). In Fig. 1, it is interesting to note that 90% of the 1 nm particles are deposited in the H region, 10% in the TB region and none in the A region. For 20 nm particles, however, 50% deposit in the A region and 25% in the H and TB regions. Here, it should be noted that the above predicted deposition curves are only suitable for workers with light exercise conditions under nose-only breathing conditions. Although they were adequate to predict carbon black workers based on our field observations, they are not suitable for workers with other working conditions. For workers with other work loads, it is suggested to predict lung depositions by using the measured size distributions of nanoparticles obtained MEAD,

then apply them to UK National Radiological Protection Board's (NRPB's) LUDEP Software according to the work load found in the field.

Results and Discussion

Size distributions of nanoparticles obtained from the three selected workplaces using the MEAD. Table 1 shows the size distributions of nanoparticles (measured particle size range: 1–1000 nm) obtained from the three selected workplaces. It can be seen that the count median diameter (CMD) and the corresponding standard deviation (σ_g) of the outdoor background were 48.3 nm and 1.78, respectively. The above results were quite similar to those workplace backgrounds obtained from the packing area (CMD = 42.7 nm, σ_g = 1.84) and warehouse (CMD = 41.1 nm, σ_g = 2.04) indicating background nanoparticle concentrations of both workplaces were mainly coming from outdoor atmosphere. The above inference was consistent with the results conducted by Wake (*31*).

In the present study, we found that all resultant size distributions for workplace exposures were consistently in a bi-model form (as shown Fig. 2 for illustration). For the first mode, we found that the CMD and the corresponding σ_g were 25.5 nm and 3.1, 24.2 nm and 1.8, and 39.2 nm and 3.2 for the packaging area, warehouse, and pelletizing area, respectively (Table 1). In principle, these nanoparticles could be coming from the carbon black aggregates. However, according to the results conducted by Kuhlbusch et al. in three carbon black manufacturing plants and based on our field observation, that nanoparticles of this size range found in the warehouse and pelletizing area could be also contributed by the exhaust of the forklift and fugitive emissions of heaters, respectively (*25-26*). In principle, carbon black, forklift exhaust and heater fugitive are carbon-containing materials. Although they are intrinsically different in their chemical compositions (such as organic carbon, inorganic carbon, trace metal contents…), they are soot in nature and have very similar size distributions. The above characteristics lead to difficulties in collecting each individual pollutant in the field. Therefore, we did not further characterize each individual concentration of these three pollutants.

For nanoparticles of the second mode, we found that size distributions in both the packaging area (CMD = 165 nm, σ g = 2.1) and warehouse (CMD = 166 nm, σ g = 2.2) were quite similar and both were coarser that that of pelletizing area (CMD = 124 nm, σ g = 2.0) (Table 1). Based on our field observation, we found that a total enclosure device was used for the pelletizing process. Therefore, the emissions of nano-carbon black from the pelletizing process could be mainly contributed by the duct fugitives governed by the thermal lifting draft. On the other hand, the emissions of nano-carbon black from both the packaging area and warehouse were mainly due the agitation of carbon blacks during the packaging and shipping processes. Based on the above observations, it is not so surprising to see that particle size distributions in both the packaging area and warehouse were quite similar and both were coarser that that of pelletizing area.

Number concentrations and surface area concentrations of nanoparticles obtained from the three selected workplaces using MEAD. Table 2 shows the number and surface area concentrations of nanoparticles (measured particle size range: 1−1000 nm) for the outdoor background, the three selected workplace exposures and their corresponding workplace backgrounds. For number concentrations, no significant difference can be found between the concentrations of the outdoor background (mean = 3.41×10^3 #/cm^3) and that of the workplace background concentrations of the packaging area (mean = 3.46×10^3 #/cm^3) (*t*-test; $p>0.05$), but both was slightly lower than that of the workplace background concentration of the warehouse (18.62×10^3 #/cm^3) (*t*-test; $p<0.05$). According to the inference made in the previous section (based on measured size distributions), the background concentrations of the above two workplaces could be mainly coming from outdoor atmosphere. Obviously, the number concentration results obtain from the packaging area do support the above inference. The inconsistency found in the warehouse is warrant the need for further discussion. Based on our field observation, we found that the warehouse had only one side open during the daytime for the shipping purpose, and the warehouse was totally enclosed during the night time. Therefore, the high background number concentration found in warehouse could be due to the accumulative effect. On the other hand, we found the manual packaging area always has two sides open in both day- and

night-time. The above observation might explain why its background number concentrations were quite similar to that of outdoor atmospheric environment.

In this study, we found that the number concentrations of workplace exposures obtained from the packaging area (mean = 25.7×10^3 #/cm^3) was consistent with that obtained from Wake ($4–50\times10^3$ #/cm^3) (*31*). Moreover, we also found that the number concentrations for both packaging area and warehouse (mean = 25.7×10^3 and 42.13×10^3 #/cm^3, respectively) were significantly higher than their corresponding workplace background concentrations (=3.46×10^3 and 18.62×10^3 #/cm^3, respectively) (*t*-test; $p<0.05$). The above results clearly indicate that process emissions could effectively elevate the number concentrations of nanoparticles in workplace atmospheres. However, it also should be noted that the contributions of the background level to total nanoparticle exposure for the above two areas were 13% and 44%, respectively. In the present study, no workplace background concentrations were measured for the pelletizing area (because it worked for 24 h per day). Nevertheless, we found that its workplace concentrations (13.71×10^3 #/cm^3) fell within the range ($8–44\times10^3$ #/cm^3) obtained from three carbon black manufacturing plants conducted by Kuhlbusch et al. (*25–26*). If the outdoor background concentration (mean = 3.41×10^3 #/cm^3) was used the reference background level, its contribution to total nanoparticle exposure of the pelletizing area was 25%.

Finally, we found that the trends found in the resultant number concentrations (as described above) can also be seen in the corresponding surface area concentrations. In the present study, no significant difference can also be found between the surface area concentrations of the outdoor background (mean = 203 μm^2/cm^3) and that of the workplace background concentrations of the packaging area (mean = 192 μm^2/cm^3) (*t*-test; $p>0.05$), but both was slightly lower than that of the workplace background concentration of the warehouse (240 μm^2/cm^3) (*t*-test; $p<0.05$). Moreover, we also found that the surface area workplace exposure concentrations for both packaging area and warehouse (mean = 782 μm^2/cm^3 and 1195 μm^2/cm^3, respectively) were significantly higher than their corresponding workplace background concentrations (=192 and 240 μm^2/cm^3, respectively) (*t*-test; $p<0.05$). We also found that the workplace exposure concentrations of the pelletizing area (441

256 $\mu m^2/cm^3$) were significantly lower than that of the packaging area and warehouse (=782 $\mu m^2/cm^3$
257 and 1195 $\mu m^2/cm^3$, respectively) (*t*-test; $p<0.05$).

258 **Estimating number and surface area concentrations of nanoparticles deposited on different**
259 **regions of the respiratory tract.** In this study, the resultant size distribution data was further used to
260 estimate both the number concentrations and surface area concentrations of nanoparticles deposited
261 on different regions of the respiratory tract for the three selected workplaces. Table 3 shows the
262 estimated number concentrations (and their percents) deposited on the three regions of the H, TB, and
263 A of the respiratory tract. For the packaging area, the estimated number concentrations for the H, TB,
264 and A regions were 4.98×10^3 #/cm^3, 4.45×10^3 #/cm^3, and 16.4×10^3 #/cm^3, respectively. For the
265 warehouse were 6.79×10^3 #/cm^3, 7.18×10^3 #/cm^3, and 28.3×10^3 #/cm^3, respectively. For the
266 pelletizing area were 2.08×10^3 #/cm^3, 2.35×10^3 #/cm^3, and 9.47×10^3 #/cm^3, respectively. The percent
267 of nanoparticles deposited on the three regions, while presented in sequence, were: (1) packaging area:
268 A (64%) > H (19%) > TB (17%), (2) warehouse: A (67%) > TB (17%) > H (16%), and (3) pelletizing
269 area: A (68%) > TB (17%) > A (15%). The above results clearly indicate that the fractions of
270 nanoparticles deposited on the A region were much higher than that of the other two regions for all
271 selected workplaces.

272 Table 4 shows the estimated surface area concentrations (and their percents) deposited on the three
273 regions of the H, TB, and A of the respiratory tract for the three selected workplaces. For the
274 packaging area, the estimated surface area concentrations for the H, TB, and A regions were 62.6
275 $\mu m^2/cm^3$, 93.8 $\mu m^2/cm^3$, and 625 $\mu m^2/cm^3$, respectively. For the warehouse, they were 35.9
276 $\mu m^2/cm^3$, 155 $\mu m^2/cm^3$, and 1,003 $\mu m^2/cm^3$, respectively. For the pelletizing area, they were 8.82
277 $\mu m^2/cm^3$, 57.3 $\mu m^2/cm^3$, and 374 $\mu m^2/cm^3$, respectively. The percent of nanoparticles deposited on
278 the three regions, while presented in sequence, shared the same trend as: (1) packaging area: A (80%)
279 > TB (12%) > H (8%), (2) warehouse: A (84%) > TB (13%) > H (3%), and (3) pelletizing area: A
280 (85%) > TB (13%) > H (2%).

By comparing the results shown in Table 3 and Table 4, significant differences can be found in the fractions of nanoparticles deposited on each of the three regions while different exposure metrics were adopted. Our results clearly indicate the importance for simultaneously predicting both the surface area and number concentrations of nanoparticles deposited on different regions of the respiratory tract for nanoparticle exposure assessments. Here, it should be noted that surface area concentrations obtained from the present study were based on mathematical calculations assuming an isometric shape of the inhaled particles, whereas in reality materials with the same particle size can have very different specific surface areas, depending on porosity, fractal dimension, etc. Although the surface area of nanoparticles can be determined via many different methods (such as BET, epiphaniometer, and LQ1-DC), different methods might result in different surface area concentrations. Though the real nanoparticle surface area could not be obtained, we assume the results obtained from the present study (assuming an isometric shape of the inhaled particles) would be proportional to real values and could be able to, at least, relate to their resultant health outcomes.

Confirmation of MEAD results. In principle, the MEAD can be used to directly estimate both the number and surface area concentrations of nanoparticles deposited on different regions of the respiratory tract (including H, TB and A regions) (*18*). However, the aforementioned equipment has never been used in the field. Therefore, the applicability of MEAD in the workplace is still required further confirmation.

Fig. 3 compares the results of the surface area concentrations deposited on both the TB and A regions obtained from MEAD with that obtained from NSAM. For the TB region, the results obtained from the NSAM for the packaging area, warehouse, and pelletizing area were 96.2 $\mu m^2/cm^3$, 154 $\mu m^2/cm^3$, and 55.3 $\mu m^2/cm^3$, respectively. The above results were quite comparable to those obtained from MEAD (= 93.8 $\mu m^2/cm^3$, 155 $\mu m^2/cm^3$, and 57.3 $\mu m^2/cm^3$, respectively) (*paired* *t*-test, $p>0.05$). The same trend can also be found for that of the A region (NSAM = 700 $\mu m^2/cm^3$, 1,208 $\mu m^2/cm^3$, and 398 $\mu m^2/cm^3$, respectively; and MEAD = 625 $\mu m^2/cm^3$, 1,003 $\mu m^2/cm^3$, and 374 $\mu m^2/cm^3$, respectively) (*paired* *t*-test, $p>0.05$). As shown in Fig. 3, both NSAM and MEAD

results obtained from the warehouse were found with higher variations than that obtained from the other two workplaces. Based on our field observation, the higher variations found in the warehouse might because high variations of forklift used in the warehouse during the sampling periods. Considering both NSAM and MEAD sharing the same measuring principles (i.e., particle charging efficiency and particle electrical mobility), comparable results obtained from both instruments could be theoretically plausible.

In the present study, although significant differences can be found in the magnitude of the measured values obtained from MEAD and that obtained SMPS (*paired t*-test, $p<0.05$), a good correlation ($r = 0.92$) can be found between them (data not shown). In particular, values obtained from the MEAD were consistently higher than that from SMPS. Considering measuring principles of the MEAD was different from that of SMPS, the existence of systemic differences between their measured results could be theoretically plausible. The same scenario has also been found in a study conducted by Woo et al. while different instruments were used to measure atmospheric nanoparticle concentrations (*15*). In this study, the results obtained from the SMPS were used as the reference to normalize the values obtained from the MEAD. Then, no significant difference can be found between these measured values (after being normalized) (*paired t*-test, $p>0.05$) (Fig. 4). The relationship between the measured surface area concentrations obtained from SMPS (i.e., x) and their corresponding normalized surface area concentrations obtained from MEAD (i.e., y) were found as: $y = 1.05x$ ($n= 12$, $R^2= 0.81$). The above results indicate that the MEAD is suitable for nanoparticle exposure assessments in the field. In our previous study, Li et al. used materials with dielectric constants ranging from 2.5 to infinite for the correction between the EAD readouts (at 20 V ion-trap voltage) and the calculated particle surface area concentrations deposited in TB and A regions. We found that the variations were ~13% and 5%, respectively (*19*). We also found that the increase in ion-trap voltage would reduce the dielectric effect on EAD readouts. In the present study, the dielectric constant of carbon black was found ranging from 2.5 to 3.0, and the ion-trap voltages were set ranging from 20 to 2500 voltage indicating the effect of the materials property on MEAD readouts

might become less significant. The above results further confirm the validity MEAD results obtained from the present study.

We found that workplace background nanoparticle concentrations for both packaging area and warehouse workplaces were mainly coming from outdoor atmosphere. Size distributions of nanoparticles of workplace exposures were consistently in the form of bi-model for the three selected process areas. The first mode could be contributed not only by the process emissions, but also exhaust of the forklift or fugitive emissions of heaters. On the other hand, nanoparticles of the second mode were mainly from the emissions of nano-carbon black from the process areas. For both number and surface area concentrations, the fractions of nanoparticles deposited on the A region were much higher than that of the two regions of the TB and H for all selected workplaces. However, significant differences was found in the percents of nanoparticles deposited on each of the three regions of the respiratory tract while different exposure metrics were adopted. Our results clearly indicate the importance for simultaneously predicting both the surface area and number concentrations of nanoparticles deposited on different regions of the respiratory tract for nanoparticle exposure assessments. In the present study, results obtained from both NSAM and MEAD were quite comparable. In addition, no significant difference can be found between the measured values obtained from SMPS and the corresponding MEAD values after being normalized. Considering the intrinsic advantages of MEAD (i.e., less expensive, less bulky, and easy to use), our results further support the suitability of using MEAD in the field for nanoparticle exposure assessments. Nevertheless, it also should be that the newly developed MEAD cannot be regarded as a replacement for SMPS particularly when the number concentrations are lower than 10^2–10^3 #/cm^3.

Acknowledgment

We are grateful to the Institute of Occupational Safety and Health (IOSH) in Taiwan for funding this research project.

Literature Cited

(1) Peters, A.; Wichmann, H. E.; Tuch, T.; Heinrich, J.; Heyder, J. Respiratory effects are associated with the number of ultrafine particles. *Am. J. Respir. Crit. Care Med.* **1997**, 155, 1376–1383.

(2) Kreyling, W. G.; Semmler, M.; Erbe, F.; Mayer, P.; Takenaka, S.; Schulz, H. Translocation of ultrafine insoluble iridium particles from lung epithelium to extrapulmonary organs is size dependent but very low. *J. Toxicol. Environ. Health*. **2002**, 65, 1513–1530.

(3) Oberdörster, G. Pulmonary effects of inhaled ultrafine particles. *Int. Arch. Occup. Environ. Health*. **2001**, 74, 1–8.

(4) Donaldson, K.; Brown, D.; Clouter, A.; Duffin, R.; MacNee, W.; Renwick, L.; Tran, L.; Stone, V. The pulmonary toxicology of ultrafine particles. *J. Aerosol. Med.* **2002**, 15, 213–220.

(5) Dockery, D. W.; Pope, C. A.; Xu, X.; Spengler, J. D.; Ware, J. H.; Fay, M. E. An Association between air pollution and mortality in six U.S. cities. *N. Engl. J. Med.* **1993**, 329, 1753–1759.

(6) Oberdörster, G. Toxicology of ultrafine particles: in vivo studies. *Philos. Trans. R. So.c Lond A*. **2000**, 358, 2719–2740.

(7) Oberdörster, E. Manufactured nanomaterials (Fullerenes, C60) induce oxidative stress in the brain of juvenile largemouth bass. *Environ. Health Perspect*. **2004**, 112, 1058–1062.

(8) Oberdörster, G. Significance of particle parameters in the evaluation of exposure-dose-response relationships of inhaled particles. *Part. Sci. Technol.* **1996**, 14, 135–151.

(9) Donaldson, K.; Li, X. Y.; MacNee, W. Ultrafine (nanometer) particle mediated lung injury. *J Aerosol Sci*. **1998**, 29, 553–560.

(10) Tran, C. L.; Buchanan, D.; Cullen, R. T.; Searl, A.; Jones, A. D.; Donaldson, K. Inhalation of poorly soluble particles. Ⅱ. Influence of particle surface area on inflammation and clearance. *Inhal. Toxicol.* **2005**, 12, 1113–1126.

(11) Elder, A.; Gelein, R.; Finkelstein, J. N.; Driscoll, K. E.; Harkema, J.; Oberdörster, G. Effects of subchronically inhaled carbon black in three species. Ⅰ. Retention kinetics, lung inflammation, and histopathology. *Toxicol. Sci.* **2005**, 88, 614–629.

(12) Stoeger, T.; Reinhard, C.; Takenaka, S.; Schroeppel, A.; Karg, E.; Ritter, B.; Heyder, J.; Schulz, H. Instillation of six different ultrafine carbon particles indicates a surface area threshold dose for acute lung inflammation in mice. *Environ. Health Perspect*. **2006**, 114, 328–333.

(13) Brown, J. S.; Zeman, K. L.; Bennett, W. D. Ultrafine particle deposition and clearance in the healthy and obstructed lung. *Am. J. Resp. Crit. Care Med*. **2002**, 166, 1240–1247.

(14) Brouwer, D. H.; Gijsbers, J. H. J.; Lurvink, M. W. M. Personal exposure to ultrafine particles in the workplace: exploring sampling techniques and strategies. *Annual of Occupational Hygiene*. **2004**, 48, 439–453.

(15) Woo, K. S.; Chen, D. R.; Pui, D. Y. H.; Wilson, W. E. Use of continuous measurements of integral aerosol parameters to estimate particle surface area. *Aerosol Sci. Tech.* **2001**, 34, 57–65.

(16) Wilson, W. E.; Han, H. S.; Stanek, J.; Turner, J.; Chen, D. R.; Pui, D. Y. H. Use of the electrical aerosol detector as an indicator of the surface area of fine particles deposited in the lung. *J. Air & Waste Manage. Assoc.* **2007**, 57, 211–220.

(17) Fissan, H.; Trampe, A.; Neunman, S.; Pui, D. Y. H.; Shin, W. G. Rationale and principle of an instrument measuring lung deposition area. *Journal of Nanoparticle Research.* **2007**, 9, 53–59.

(18) Li, L.; Chen, D. R.; Tsai, P. J. Use of An Electrical Aerosol Detector (EAD) for Nanoparticle Size Distribution Measurement. *Journal of Nanoparticle Research.* **2009**, 11, 111–120.

(19) Li, L.; Chen, D. R.; Tsai, P. J. Evaluation of an Electrical Aerosol Detector (EAD) for the Aerosol Integral Parameter Measurement. *Journal of Electrostatics.* **2009**, 67, 765–773.

(20) Ferin, J.; Oberdörster, G.; Penney, D. P. Pulmonary retention of ultrafine and fine particles in rats. *Am. J. Respir. Cell Mol. Biol.* **1992**, 6, 535–542.

(21) Li, X. Y.; Brown, D.; Smith, S.; MacNee, W.; Donaldson, K. Shortterm inflammatory responses following intratracheal instillation of fine and ultrafine carbon black in rats. *Inhal. Toxicol.* **1999**, 11, 709–731.

(22) Koike, E.; Kobayashi, T. Chemical and biological oxidative effects of carbon black nanoparticles. *Chemosphere.* **2006**, 65, 946–951.

(23) Tin-Tin, W. S.; Yamamoto, S.; Ahmed, S.; Kakeyama, M.; Kobayashi, T.; Fujimaki, H. Brain cytokine and chemokine mRNA expression in mice induced by intranasal instillation with ultrafine carbon black. *Toxicol. Lett.* **2006**, 163(2), 153–160.

(24) IARC monographs on the evaluation of carcinogenic risks to humans: printing processes and printing inks, carbon blacks and some nitro compounds. *IARC Monogr. Eval. Carcinog. Risks Hum*. 1996, 65, 149–262.

(25) Kuhlbusch, T. A. J.; Neumann, S.; Fissan, H. Number size distribution, mass concentration, and particle composition of PM1, PM2.5, and PM10 in bag filling areas of carbon black production. *J. Occup. Environ. Hygiene*. **2004**, 1, 660–671.

(26) Kuhlbusch, T. A. J.; Neumann, S.; Fissan, H. Particle characteristics in the reactor and pelletizing areas of carbon black production. *J. Occup. Environ. Hygiene.* **2006**, 3, 558–567.

(27) NIOSH, National Institute for Occupational Safety and Health. Approaches to safe nanotechnology: An information exchange with NIOSH. **2005**.

(28) Tsai, P. J.; Shieh, H. Y.; Lee, W. J. Characterization of PAHs in the Atmosphere of Carbon Black Manufacturing Workplaces. *Journal of Hazardous Materials.* **2002**, 91, 25–42.

(29) James, A. C.; Bailey, M. R.; Dorrian, M. D. LUDEP Software Version 2.07: program for implementing ICRP-66 Respiratory tract model, RPB, Chilton, Didcot, OXON, OX11 ORQ, UK. **2000**.

(30) ICRP, International Commission on Radiological Protection. Human respiratory tract model for radiological protection, Publication 66,Annals of ICRP. Oxford, Pergamon: London, UK. **1994**.

(31) Wake, D. Ultrafine particles in the workplace. HSL Report number ECO/00/18. **2001**.

434 **Captions**

435 **Figures**

436 FIGURE 1. Calculated deposition curves of nanoparticles for the head airway (H), tracheobronchial
437 (TB), and alveolar (A) regions of the respiratory tract

438 FIGURE 2. MEAD measured size distribution (in particle number) obtained from the package area

439 FIGURE 3. Comparing surface area concentrations of nanoparticles deposited on (a) TB region and
440 (b) A region measured by the MEAD with that measured by the NSAM

441 FIGURE 4. Comparing surface area concentrations obtained from SMPS with that from MEAD
442 after being normalized

443

444 **Tables**

445 TABLE 1. Number-based size distributions of nanoparticles (1–1000 nm) obtained from MEAD for
446 the outdoor atmospheric background, workplace background, and workplace atmosphere
447 of the three selected process areas (n= 4)

448 TABLE 2. Number concentrations and surface area concentrations of nanoparticles (1–1000 nm) for
449 the three selected process areas (n= 4)

450 TABLE 3. Number concentrations of nanoparticles (1–1000 nm) deposited on the H, TB, and A
451 regions of the respiratory tract for the three selected process areas (n= 4)

452 TABLE 4. Surface area concentrations of nanoparticles (1–1000 nm) deposited on the H, TB, and A
453 regions of the respiratory tract for the three selected process areas (n= 4)

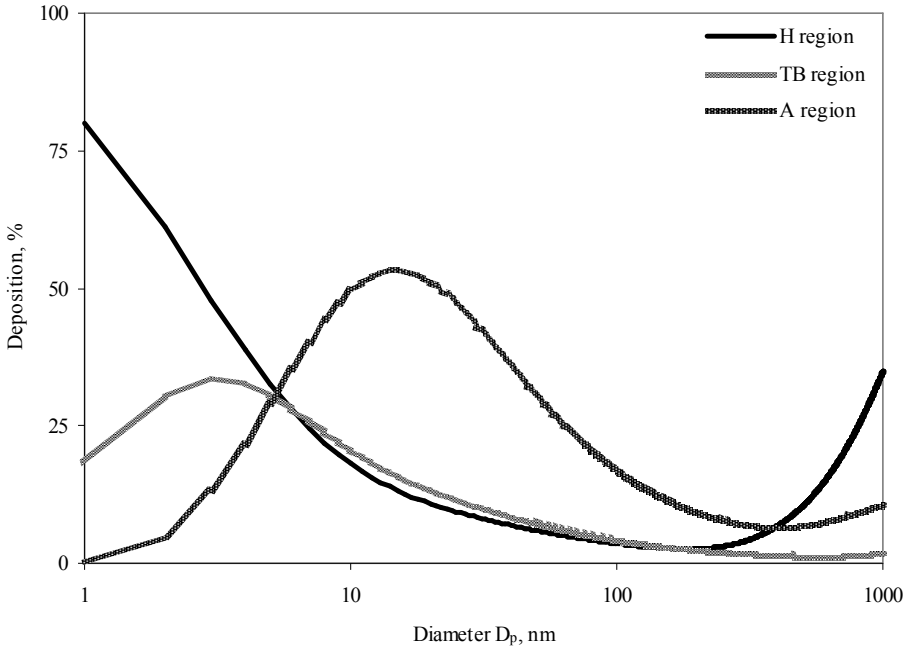

FIGURE 1. Calculated deposition curves of nanoparticles for the head airway (H), tracheobronchial (TB), and alveolar (A) regions of the respiratory tract using the LUDEP model software

473

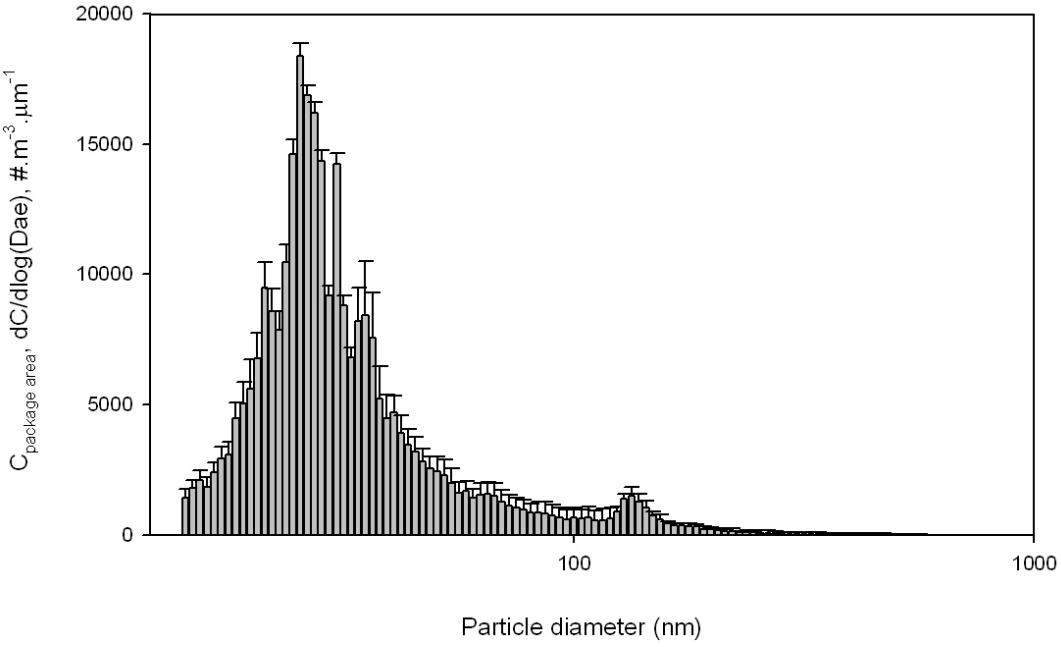

474

475 FIGURE 2. MEAD measured size distribution (in particle number) obtained from the package area

476

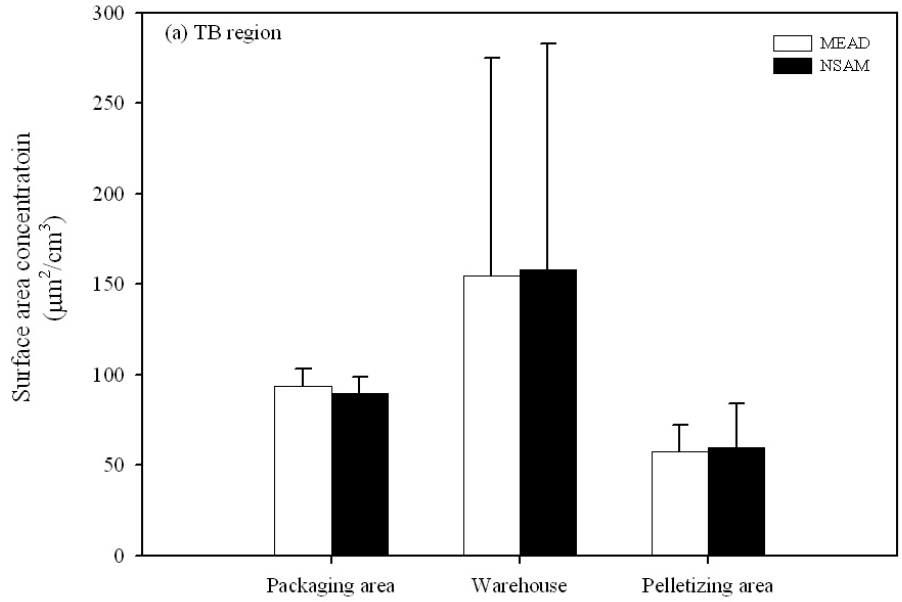

477

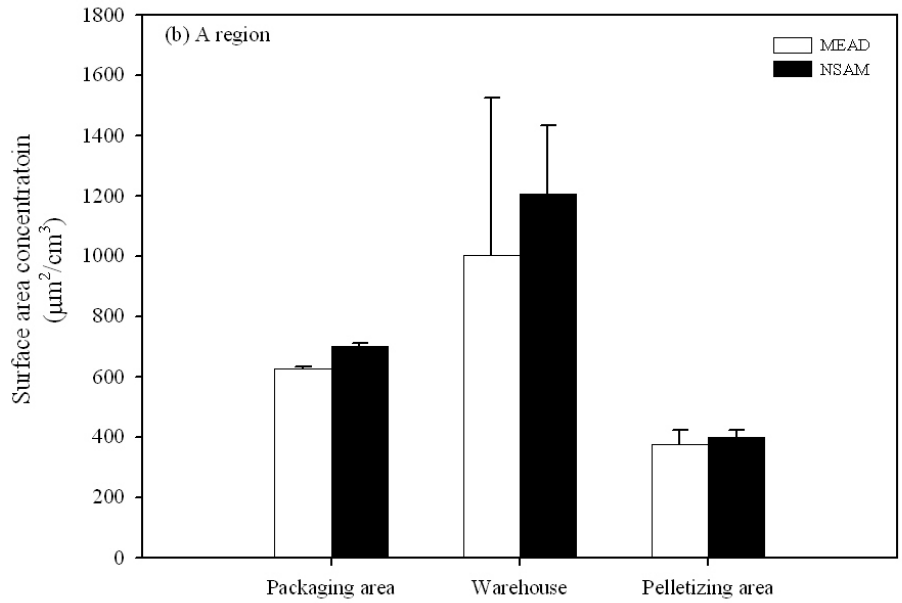

478

479 FIGURE 3. Comparing surface area concentrations of nanoparticles deposited on (a) TB region and
480 (b) A region measured by the MEAD with that measured by the NSAM

481

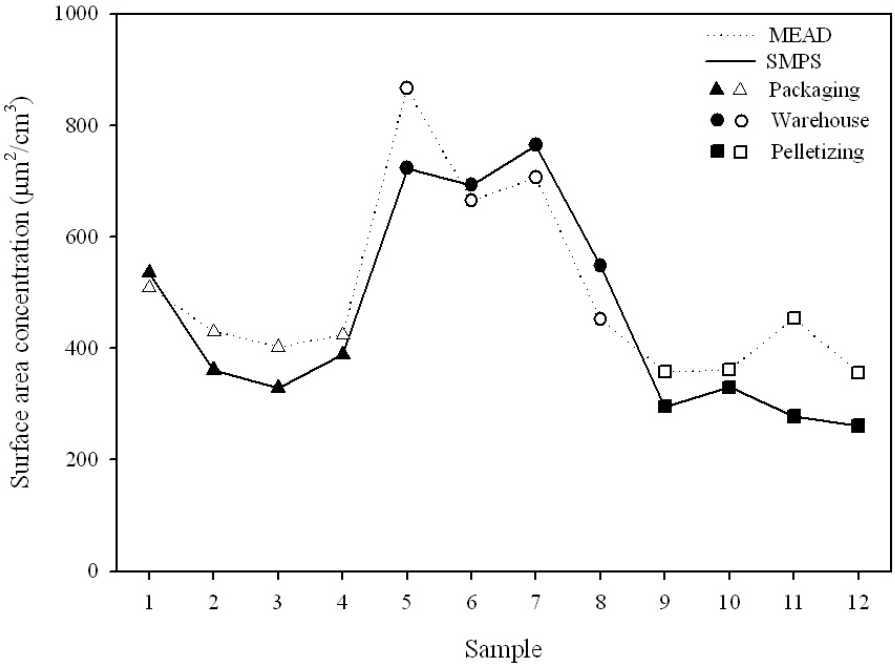

482

483 FIGURE 4. Comparing surface area concentrations obtained from SMPS with that from MEAD
484 after being normalized

485

TABLE 1. Number-based size distributions of nanoparticles (1–1000 nm) obtained from MEAD for the outdoor background, workplace background, and workplace exposure of the three selected process areas (n= 4)

Sampling site	Outdoor background		Workplace background		Workplace exposure			
					1st mode		2nd mode	
	CMD (nm)	σ_g	CMD (nm)	σ_g	CMD (nm)	σ_g	CMD (nm)	σ_g g
Packaging			42.7	1.84	25.5	3.1	165	2.1
Warehouse	48.3	1.78	41.1	2.04	24.2	1.8	166	2.2
Pelletizing			NM[a]	NM[a]	39.2	3.2	124	2.0

[a]NM = Not measured

TABLE 2. Number concentrations and surface area concentrations of nanoparticles (1–1000 nm) for the three selected process areas (n= 4)

Sampling site	Number concentration (#/cm^3 ×10^3)			Surface area concentration (μm^2/cm^3)		
	Outdoor background	Workplace background	Workplace exposure	Outdoor background	Workplace background	Workplace exposure
Packaging		3.46	25.7		192	782
Warehouse	3.41	18.6	42.1	203	240	1195
Pelletizing		NM[a]	13.7		NM[a]	441

[a]NM = Not measuremen

TABLE 3. Number concentrations and their corresponding fractions (values in parentheses) of nanoparticles (1–1000 nm) deposited on the H, TB, and A regions of the respiratory tract for the three selected process areas (n= 4)

Sampling site	Total (#/cm^3×10^3)	Number concentrations (#/cm^3×10^3)		
		H	TB	A
Packaging	25.7 (100%)	4.98±3.03 (19%)	4.45±2.71 (17%)	16.4±13.0 (64%)
Warehouse	42.1 (100%)	6.79±6.64 (16%)	7.18±7.66 (17%)	28.3±44.4 (67%)
Pelletizing	13.7 (100%)	2.08±0.29 (15%)	2.35±0.28 (17%)	9.47±1.09 (68%)

TABLE 4. Surface area concentrations and their corresponding fractions (values in parentheses) of nanoparticles (1–1000 nm) deposited on the H, TB, and A regions of the respiratory tract for the three selected process areas (n= 4)

Sampling site	Total (μm^2/cm^3)	Number concentrations (μm^2/cm^3)		
		H	TB	A
Packaging	782 (100%)	62.6±14.2 (8%)	93.8±1.97 (12%)	625±9.55 (80%)
Warehouse	1195 (100%)	35.9±515 (3%)	155±124 (13%)	1003±523 (84%)
Pelletizing	441 (100%)	8.82±9.12 (2%)	57.3±13.7 (13%)	374±49.4 (85%)